Pioglitazone increases VEGFR3 expression and promotes activation of M2 macrophages via the peroxisome proliferator-activated receptor γ

CONGHUI ZHANG[1], YING ZHANG[1], CHUNXIU ZHANG[1], YANG LIU[2], YANYAN LIU[1] and GANG XU[1]

[1]Department of Nephrology, Tongji Hospital, Tongji Medical College,
Huazhong University of Science and Technology, Wuhan, Hubei 430030; [2]Department of Orthopedics,
Tianjin Medical University General Hospital, Heping, Tianjin 300070, P.R. China

Abstract. The peroxisome proliferator-activated receptor γ (PPARγ) agonist pioglitazone has been widely used in previous studies to ameliorate diabetes mellitus and regulate inflammation. However, the present study aimed to investigate the effect of pioglitazone on macrophages and determine its impact on renal fibrosis *in vivo*. Firstly, bone marrow-derived macrophages (BMDM) were used to detect the effects of pioglitazone on macrophages *in vitro*. It was demonstrated that pioglitazone promoted M2 macrophage activation and induced vascular endothelial growth factor receptor 3 (VEGFR3) upregulation in a PPARγ-dependent manner. Furthermore, pioglitazone increased macrophage proliferation and macrophage VEGFR3 expression in a murine unilateral ureteral obstruction (UUO) model; however, it had no therapeutic effect on renal fibrosis *in vivo*. Therefore, the results in the present study implied that presence of M2 macrophages may inhibit pioglitazone's ability to attenuate UUO-induced renal fibrosis. In addition, the results demonstrated that macrophage-associated VEGFR3 could be induced by pioglitazone, although it is still unclear what role VEGFR3+ M2 macrophages have in renal fibrosis.

Introduction

Chronic kidney disease (CKD) is a progressive loss in kidney function over a period of months or years. There is a high global prevalence of CKD, which imposes an enormous socioeconomic burden on individuals with the disease and society (1-3). Renal fibrosis is thought to be the common final outcome of almost all CKD (4). In the present study, a murine unilateral ureteral obstruction (UUO) model was used to generate renal fibrosis *in vivo* (5).

Macrophages are important immune cells, which can be divided into two main subtypes, namely M1 and M2. They serve a crucial role under both pathological and physiological conditions. In the context of kidney disease, M1 macrophages have been demonstrated to exert a pathogenic function in renal inflammation and may represent a possible therapeutic target (6). M2 macrophages appear to suppress inflammation and promote injury repair; therefore, representing a potential treatment for renal disease. However, M2 macrophages may also function as a fibrosis promoter (7). Studies have indicated that targeting macrophages, including macrophage depletion, disruption of macrophage recruitment and genetic alteration of macrophage activity, may be used as novel therapeutic approaches in a range of diseases (8,9), including inflammation and cancer.

Peroxisome proliferator-activated receptor γ (PPARγ), which forms a heterodimer with the retinoid X receptor on peroxisome response elements, is a ligand-activated transcription factor that regulates glucose and lipid metabolism, immune responses, and inflammation (10). PPARγ is expressed in several cell types, including immune cells and various epithelial and muscle-like cells (10). The PPARγ agonist pioglitazone is used worldwide to treat patients with diabetes (11). Pioglitazone takes part in several physiopathologic processes, including glucose metabolism, lipogenesis, inflammation, proliferation, apoptosis and fibrosis, vascular reactivity (12). A previous study demonstrated that macrophage PPARγ was necessary for accelerating pioglitazone-mediated recovery from dextran sodium sulfate colitis (13). However, the specific mechanisms underlying the effect of pioglitazone on macrophages requires further study.

In the present study, the aim was to determine whether pioglitazone may influence macrophages through PPARγ and to investigate its role on renal fibrosis *in vivo*.

Materials and methods

Cells and reagents. Bone marrow cells were obtained by flushing the femurs and tibias of normal male C57/BL6 mice in Dulbecco's modified Eagle's medium (DMEM; GE

Correspondence to: Professor Yanyan Liu or Professor Gang Xu, Department of Nephrology, Tongji Hospital, Tongji Medical College, Huazhong University of Science and Technology, 1095 Jiefang Avenue, Wuhan, Hubei 430030, P.R. China
E-mail: liuyy1919@163.com
E-mail: xugang@tjh.tjmu.edu.cn

Healthcare Life Sciences, Logan, UT, USA) supplemented with 10% fetal bovine serum (FBS; Gibco; Thermo Fisher Scientific, Inc., Waltham, MA, USA) and 30% L929 conditioned medium at 37°C. The medium was changed at day 3 and day 5. L929 conditioned medium was the supernatant from growing L929 cells in DMED-containing 10% FBS for 5 days. After 7 days incubation, bone marrow-derived macrophages (BMDMs, M0) were harvested. 100 ng/ml lipopolysaccharide (LPS) and 6 ng/ml interferon (IFN)-γ were used to stimulate M0 and M1 macrophages which were harvested after 24 h. In addition, M2 macrophages were induced by stimulating M0 macrophages with 10 ng/ml interleukin (IL)-4 and 10 ng/ml IL-13 for 24 h. IL-4, IL-13, LPS and IFN-γ were purchased from PeproTech, Inc. (Rocky Hill, NJ, USA).

Pioglitazone and PPARγ antagonist GW9662 were purchased from Sigma-Aldrich (Merck KGaA, Darmstadt, Germany). M0 macrophages were stimulated with pioglitazone (5 μm) for 24 h in the presence or absence of GW9662. PPARγ inhibitor GW9662 (5 μm) was added 6 h before treatment with pioglitazone.

Western blot analysis. Cells and mouse kidney tissues were lysed using radio immunoprecipitation assay buffer containing a protease inhibitor cocktail (Wuhan Saiweier Biotechnology Co., Ltd., Wuhan, China) on ice for 30 min, then centrifuged at 16,500 x g for 30 min at 4°C to collect the supernatant. Protein concentration was quantified by a BCA protein assay kit (Beyotime Institute of Biotechnology, Shanghai, China). A total of 20 μg protein was separated by 10% SDS-PAGE and transferred to polyvinylidene fluoride membranes (EMD Millipore, Billerica, MA, USA). The membranes containing cellular protein were blocked with 5% bovine serum albumin (BSA; Sigma-Aldrich; Merck KGaA) for 1 h at room temperature. Then they were incubated overnight at 4°C with rabbit anti-arginase1 (Arg1; cat. no. sc-20150; 1:400; Santa Cruz Biotechnology, Inc., Dallas, TX, USA), rabbit anti-vascular endothelial growth factor receptor 3 (VEGFR3; cat. no. sc-321; 1:400; Santa Cruz Biotechnology, Inc.), mouse anti-inducible nitric oxide synthase (iNOS; cat. no. sc-7271; 1:200; Santa Cruz Biotechnology, Inc.) and rabbit anti-α-tubulin (1:5,000; cat. no. ab18251; Abcam, Cambridge, MA, USA). The membranes containing tissue protein were incubated overnight at 4°C with rabbit anti-α-smooth muscle actin (SMA; cat. no. ab5694; 1:1,000; Abcam), rabbit anti-platelet-derived growth factor receptor (PDGFR)-β (cat. no. ab32570; 1:1,000; Abcam), rabbit anti-PPARγ (cat. no. AP20705a; 1:1,000; Abgent, Inc., San Diego, CA, USA), rabbit anti-phosphorylated (p)-PPARγ (cat. no. ab195925; 1:1,000; Abcam) and mouse anti-GAPDH (1:3,000; Abcam; cat. no. ab8245). Following cultivated with goat anti-rabbit or goat anti-mouse secondary antibodies (1:10,000; cat. no. A27036SAMPLE; cat. no. A28177SAMPLE; Thermo Fisher Scientific, Inc., Waltham, MA, USA) at 37°C for 1 h, membranes were incubated with horseradish peroxidase (HRP)-conjugated immunoglobulin G (1:5,000; cat. no. 323065021; Jackson ImmunoResearch Laboratories, Inc., West Grove, PA, USA) for 1 min at room temperature. The protein bands were detected using a ChemiDOC™ XRS+ system (Bio-Rad Laboratories, Inc., Hercules, CA, USA). Densitometric analysis was performed using Image Lab™ software version 6.0.1(Bio-Rad Laboratories, Inc).

UUO mouse model. MaleC57/BL6 mice (n=18, weight 20-22 g; age, 6-8 weeks) were obtained from the Hua Fukang Experimental Animal Center (Beijing, China) and housed at the animal facilities at Tongji Medical Collage in an air-controlled room (temperature 23±1%, humidity 55±5%) under a 12-h light/dark cycle with free access to standard food and water. All the animal raising and handling protocols approved by the Institutional Animal Care and Use Committee of Tongji Medical College, Huazhong University of Science and Technology. The study was approved by the Ethics Committee of Tongji Hospital, Tongji Medical College, Huazhong University of Science and Technology (Wuhan, China). Animals were divided into three groups: Sham group (n=4), UUO group (n=7) and UUO + pioglitazone group (n=7). The UUO renal fibrosis model was induced as previously described (14). Briefly, an incision was made in the midline of the abdomen, and the left proximal ureter was exposed and was ligated at two separate locations using 4-0 silk suture. Mice in the sham group underwent the same surgical procedures except for ligation. The sham and UUO groups were administered a daily oral gavage of saline, whereas the UUO + pioglitazone group received 20 mg/kg pioglitazone. The dose of pioglitazone was determined according to previous studies (14). Subsequently, mice were sacrificed 14 days after UUO operation. Kidneys were excised, fixed with 4% paraformaldehyde 24 h in room temperature, then dehydrated in a graded series of alcohol (Wuhan Goodbio Technology Co., Ltd., Wuhan, China) and finally embedded in paraffin (Wuhan Goodbio Technology Co., Ltd.) as previously described (15).

Immunofluorescence staining. The 3 μm paraffin sections were treated with xylene and hydrated with graded ethanol. Following incubation with 10 mM sodium citrate buffer (pH 6) at 100°C for 20 min for antigen revival, the sections were blocked with normal goat serum (cat. no. ab7481; Abcam) for 20 min at room temperature as previously described (15). Subsequently, sections were incubated with mouse anti-F4/80 primary antibodies (cat. no. sc-377009; 1:50; Santa Cruz Biotechnology, Inc.) and rabbit anti-VEGFR3 primary antibodies (cat. no. sc-321; 1:50; Santa Cruz Biotechnology, Inc.) at 37°C for 120 min. Alexa Fluor 488- or Cy3-conjugated secondary antibodies goat anti-rabbit, or Donkey anti-mouse immunoglobulins (cat. no. GB25303/GB21401; 1:200; Wuhan Saiweier Biotechnology Co., Ltd.) were used to visualize antigen-antibody complexes at 37°C for 30 min. Nuclei were stained with DAPI at room temperature for 5 min (2 μg/ml; cat. no. D9542; Sigma-Aldrich; Merck KGaA). Digital images were captured with a fluorescent microscope (Olympus Corporation, Tokyo, Japan).

Immunohistochemistry. Following antigen retrieval with citrate buffer (pH=6.0) as above, the 3-μm paraffin sections were incubated with 3% H_2O_2 for 10 min at room temperature, and then blocked with normal goat serum (cat. no. ab7481; Abcam) for 30 min at room temperature. Sections were incubated with primary antibodies against α-SMA (cat. no. ab5694; 1:300; Abcam), F4/80 (cat. no. sc-377009; 1:50; Santa Cruz Biotechnology, Inc.) and Collagen-4 (cat. no. ab6586; 1:300; Abcam) overnight at 4°C. Then, biotinylated goat anti-rabbit secondary antibody (cat. no. GB23204; 1:100; Wuhan Saiweier
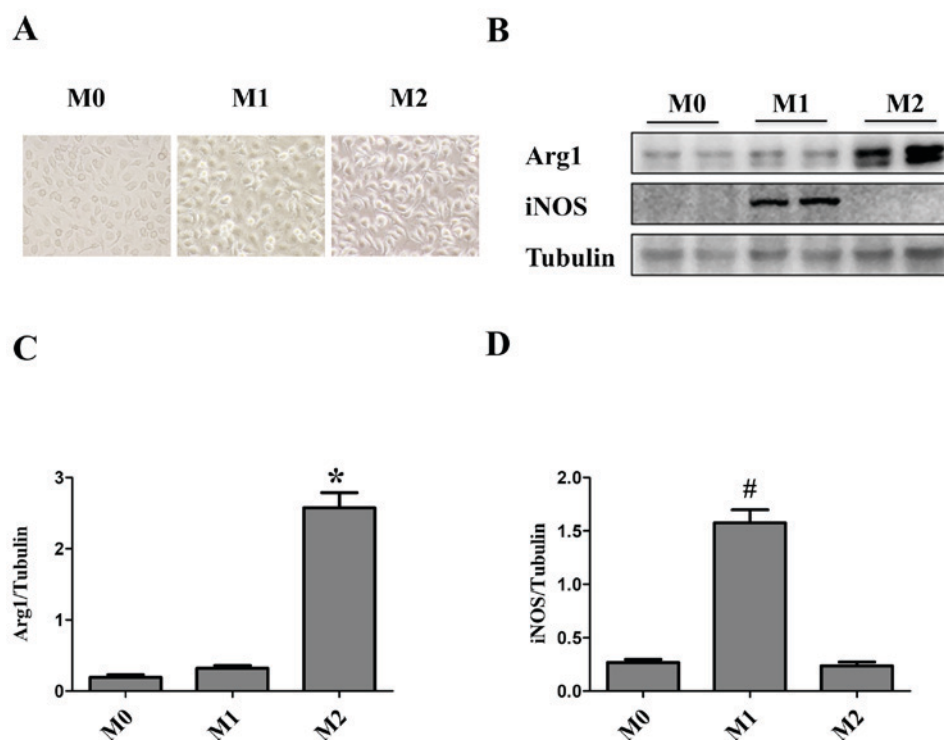
Figure 1. Identification of macrophages. Bone marrow-derived macrophages (M0) were treated for 24 h with lipopolysaccharide (100 ng/ml) + interferon-γ (6 ng/ml) to induce M1 polarization or IL-4 (10 ng/ml) + IL-13 (10 ng/ml) to induce M2 polarization. (A) Macrophage morphology was observed under phase contrast microscopy (magnification, x400): M0 macrophages were elongated and spindle-shaped, M1 macrophages were round and M2 macrophages were cone-shaped. (B) Western blot analysis was performed to determine the protein expression levels of iNOS, an M1 marker and Arg1, an M2 marker. Tubulin was used as the loading control. (C and D) Quantification of the western blot results. The data are presented as the mean ± standard error of the mean. *P<0.05 vs. M0; #P<0.05 vs. M0. Arg1, arginase1; iNOS, inducible nitric oxide synthase; M, macrophage.

Biotechnology Co., Ltd.) was used added for 30 min at room temperature followed by horseradish peroxidase-conjugated streptavidin (OriGene Technologies, Inc., Beijing, China) and 3,3'-diaminobenzidine staining (OriGene Technologies, Inc.) for several seconds at room temperature, until the sections changed to brown, when the reaction was halted with water. Digital images were captured with an optical microscope (Olympus Corporation, Tokyo, Japan).

Statistical analysis. All statistical analyses were conducted using SPSS version 12.0 (SPSS, Inc., Chicago, IL, USA). The data are expressed as the mean ± standard error of the mean from 3 independent experiments. Multiple group comparisons were performed using one-way analysis of variance followed by Dunnett's multiple comparison test. P<0.05 was considered to indicate a statistically significant difference.

Results

Identification of macrophages induced by LPS/IFN-γ and IL-4/IL-13. Macrophage maturity and subsequent polarization were confirmed by phase-contrast microscopy. Bone marrow cells were differentiated into macrophages over the course of 7 days. Initially, Macrophages were small, round and formed colonies, which were firmly adherent to the cell culture plate. Macrophage differentiation and subsequent polarization had a marked impact on cell morphology. The majority of M0 macrophages were elongated and spindle-shaped, whereas M1 macrophages were round and M2 macrophages were

cone-shaped (16) (Fig. 1A). M1 and M2 macrophages induced by LPS/IFN-γ and IL-4/IL-13, respectively, were characterized by western blot analysis. Both cell cultures were assessed for Arg1 and iNOS. iNOS protein expression levels were significantly upregulated in M1 macrophages, whereas Arg1 was significantly upregulated in M2-polarized macrophages (Fig. 1B-D).

Pioglitazone promotes M2 macrophage polarization. To identify the effect of pioglitazone on M0 to M1/M2 macrophage polarization, M0 macrophages were treated with the drug. Pioglitazone had no effect on M0 to M1 macrophage polarization according to M1 Marker iNOS (Fig. 2A and D). However, pioglitazone could polarize M0 macrophages towards an M2 phenotype. Notably, this process was not inhibited by GW9662 (a specific antagonist of PPARγ), which indicated that an alternative pathway that does not require PPARγ was involved in regulating this process (Fig. 2A-C). It was found that the expression of VEGFR3 in M0 macrophages was similar to Arg1 with pioglitazone or GW9662 (Fig. 2A and B).

Pioglitazone promotes M2 macrophage activation and upregulates VEGFR3. To explore whether pioglitazone is associated with M2 macrophage activation *in vitro*. M0 macrophages were cultured with different concentrations of pioglitazone. The western blot results demonstrated that M2 macrophage maker was increased, particularly in the 20 μM group (Fig. 3A and B). M1 macrophages activation were not be affected by pioglitazone (Fig. 3D and E). In addition, the
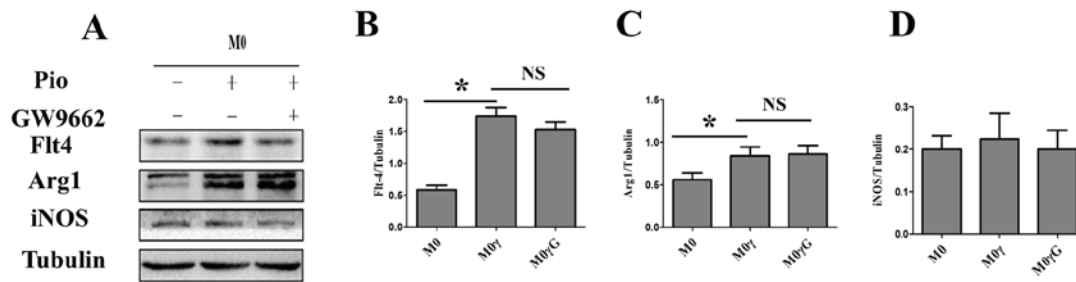
Figure 2. Pioglitazone regulates the polarization of M0 macrophages. M0 macrophages stimulated with pioglitazone (5 μm) for 24 h in the presence or absence of GW9662. PPARγ inhibitor GW9662 (5 μm) was added 6 h before treatment with pioglitazone. (A) Western blot analysis was performed to determine the protein expression levels of iNOS (M1 macrophage marker), Arg1 (M2 macrophage marker) and VEGFR3, in M0 macrophages treated with pioglitazone in the presence or absence of GW9662. Tubulin was used as the loading control. (B-D) Quantification of the western blot results. The data are presented as the mean ± standard error of the mean. *$P<0.05$. Arg1, arginase1; iNOS, inducible nitric oxide synthase; M, macrophage; M2γ, M2 treated with pioglitazone; G, GW9662; NS, not significant; Pio, pioglitazone; VEGFR3, vascular endothelial growth factor receptor 3.

protein expression levels of VEGFR3 were increased in M2 macrophages (Fig. 3C). However, this was not observed in M1 macrophages (Fig. 3F).

Pioglitazone-induced upregulation of VEGFR3 is PPARγ-dependent. Subsequently, it was investigated whether pioglitazone-induced upregulation of VEGFR3 in M2 macrophages is related to PPARγ. The results demonstrated that pioglitazone could promote M2 activation, which was inhibited by GW9662, a specific antagonist of PPARγ (Fig. 4A and B). VEGFR3 protein expression levels were increased in M2 macrophages following pioglitazone treatment, which was reversed by GW9662 (Fig. 4A and C). This confirmed that pioglitazone may enhance the expression of VEGFR3 through PPARγ.

Pioglitazone upregulates the expression of p-PPARγ and promotes macrophage proliferation of in vivo. To determine the effect of pioglitazone in vivo, a UUO mouse model was established, and the p-PPARγ and total PPARγ expression levels in the kidney tissue were measured by western blot analysis. As shown in Fig. 5A-C the total PPARγ expression levels did not change in the presence or absence of pioglitazone; however, the p-PPARγ expression levels were significantly upregulated in the UUO + pioglitazone group compared with the UUO group (Fig. 5A-B). Furthermore, pioglitazone promoted the proliferation and infiltration of macrophages (Fig. 5D).

Pioglitazone increases the expression of VEGFR3 in macrophages in vivo. To further determine whether pioglitazone could increase the expression of VEGFR3 in macrophages in vivo, double immunofluorescence staining of F4/80 and VEGFR3 was performed on kidney tissues from the sham, UUO and UUO + pioglitazone groups. In the sham group, the expression of F4/80 and VEGFR3 was low, whereas F4/80 and VEGFR3 expression levels were increased in the UUO model. Following pioglitazone treatment, the expression of F4/80 was increased, which was in line with the immunohistochemistry results. In addition, the level of VEGFR3 was greater in the UUO + pioglitazone group compared with in the UUO group, and expression was localized in the macrophages (Fig. 6).

Pioglitazone has no therapeutic effect on renal fibrosis in CKD. To further explore the therapeutic effect of pioglitazone on renal fibrosis in vivo, collagen-4, α-SMA and PDGFR-β were detected by immunohistochemistry and western blot analysis. In the sham group, α-SMA was only expressed in the small arteries (Fig. 7A). Following UUO, α-SMA was upregulated in the renal interstitium, which was not reduced by pioglitazone treatment. Collagen-4 was visible in the renal interstitium of the sham group; however, its expression was higher in the UOO group. In addition, pioglitazone treatment did not decrease collagen-4 expression in the UOO model. Western blotting also demonstrated similar results. No significant changes in protein expression levels of PDGFR-β and α-SMA were observed following pioglitazone treatment compared with UUO group, and these two proteins were lower in sham compared with the UUO group (Fig. 7B-D).

Discussion

In the present study, it was demonstrated that pioglitazone promoted the polarization of M2 macrophages. Stimulation of M2 macrophages with pioglitazone increased expression of VEGFR3, which was dependent on PPARγ. Furthermore, pioglitazone increased the expression levels of p-PPARγ in an in vivo UUO model, which was accompanied by increased infiltration of VEGFR3-expressing macrophages. However, pioglitazone did not appear to have a therapeutic effect on renal fibrosis.

Macrophages are heterogeneous populations that serve an important role in kidney homeostasis, but can also be activated to cause renal injury, or promote chronic fibrosis, when there is an ongoing renal insult (17). There are a number of mechanisms by which macrophages can promote renal fibrosis, including macrophage-to-myofibroblast transition (18,19). The present study revealed that pioglitazone promoted M0-M2 macrophage polarization, which was not mediated by PPARγ. However, pioglitazone has been identified as a high affinity ligand for PPARγ, and may also activate other PPAR subtypes, including PPARα, albeit with weak affinity (20). These discrepancies in results may be attributed to a difference in pathologic state, and further studies are required to confirm the underlying mechanisms.
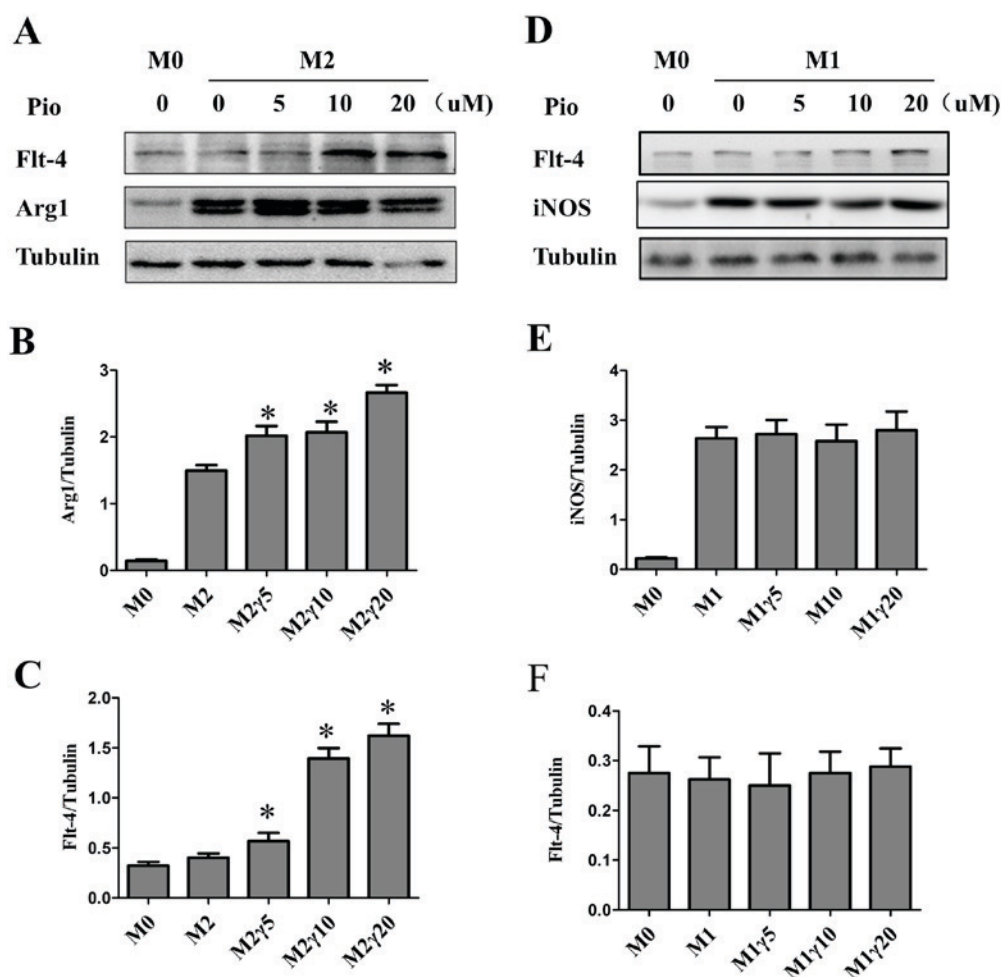
Figure 3. Effect of pioglitazone on M1 and M2 macrophages. (A) M2 and (D) M1 macrophages were treated with different concentrations of pioglitazone (0, 5, 10 and 20 μM) for 24 h and western blot analysis was performed to determine protein expression levels of VEGFR3, Arg1 and iNOS. Tubulin was used as the loading control. (B, C, E and F) Quantification of the western blot results. The data are presented as the mean ± standard error of the mean. *P<0.05 vs. M0. Arg1, arginase1; iNOS, inducible nitric oxide synthase; M, macrophage; Pio, pioglitazone; VEGFR3, vascular endothelial growth factor receptor 3.
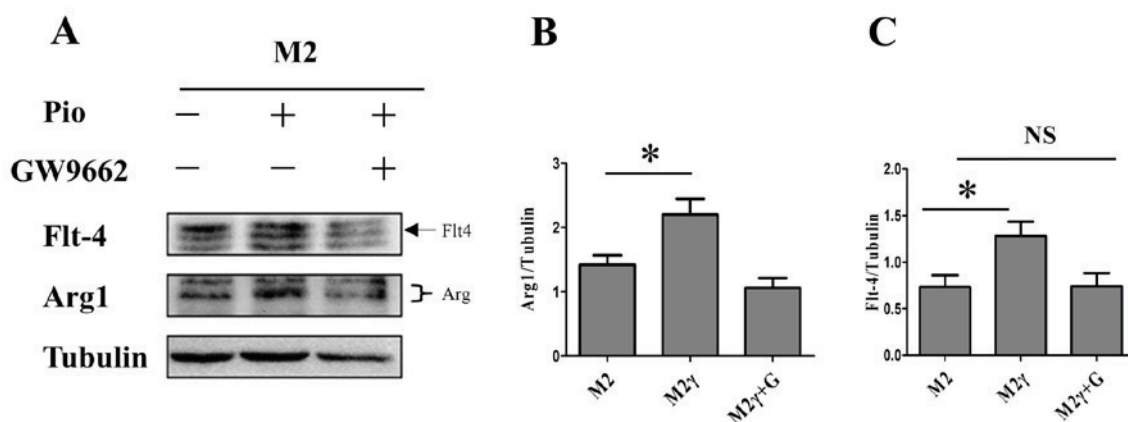

Figure 4. Pioglitazone upregulates VEGFR3 expression in M2 macrophages via peroxisome proliferator-activated receptor γ. (A) M2 macrophages were treated with pioglitazone in the presence or absence of GW9662, and western blot analysis was performed to determine the protein expression levels of Arg1 and VEGFR3. Tubulin was used as the loading control. (B and C) Quantification of the western blot results. The data are presented as the mean ± standard error of the mean. *P<0.05 vs. M2. Arg1, arginase1; M, macrophage; NS, not significant; Pio, pioglitazone; M2γ, M2 treated with pioglitazone; G, GW9662; VEGFR3, vascular endothelial growth factor receptor 3.

Furthermore, pioglitazone enhanced the activation in M2 macrophages by activating PPARγ, which was consistent with a previous study where BMDM were co-cultured with cancer cells (21). Pioglitazone has a strong ability to promote proliferation and infiltration of macrophages *in vivo*, which may promote fibrogenic activities (22).
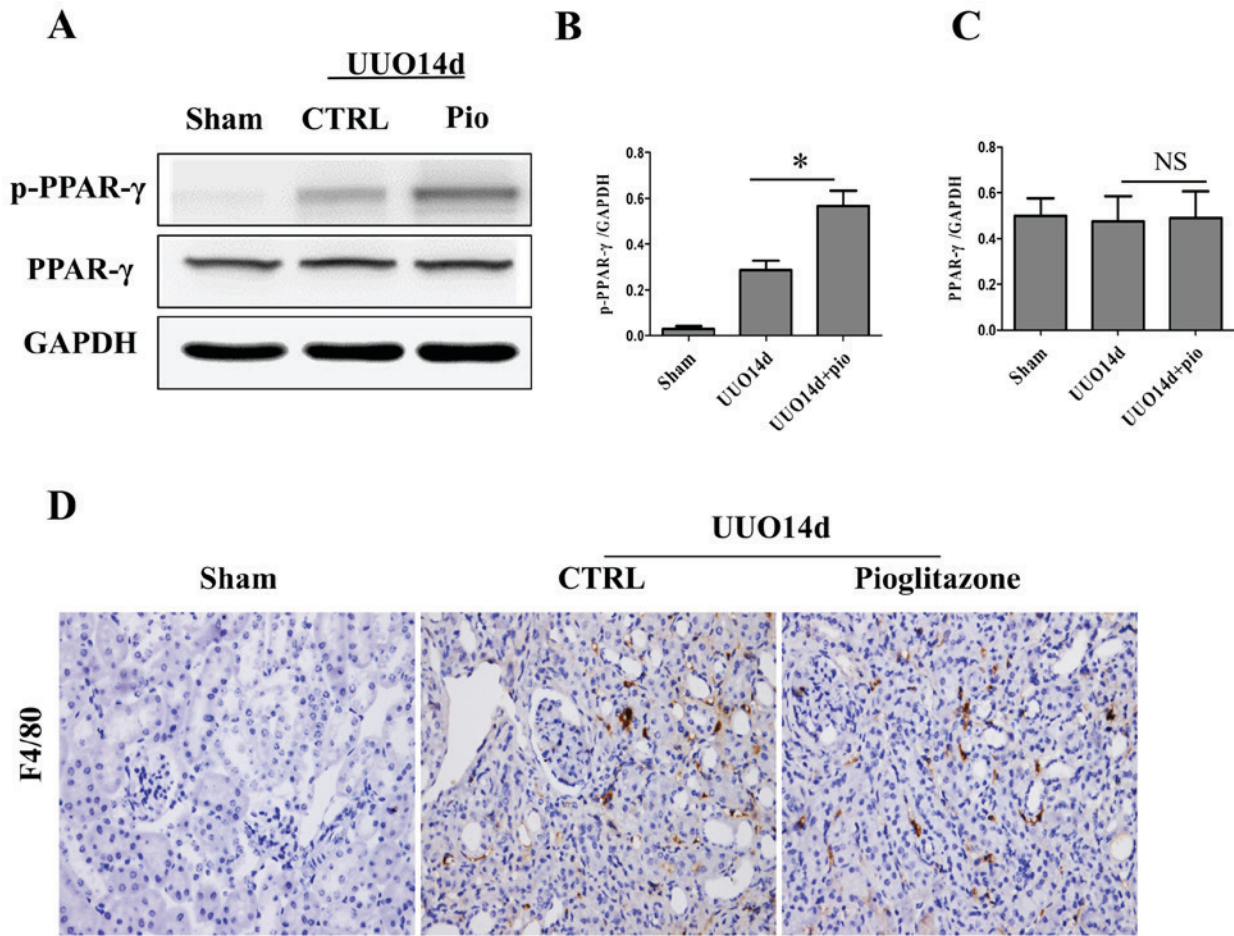
Figure 5. Pioglitazone affects p-PPARγ expression and macrophage proliferation *in vivo*. (A) Western blot analysis of total PPARγ and p-PPARγ protein expression following pioglitazone treatment in an *in vivo* UUO model. GAPDH was used as the loading control. (B and C) Quantification of the western blot results. (D) Immunohistochemical staining of F4/80 in kidney tissues of mice in the sham, UUO and UUO + pioglitazone groups. Scale bar=100 μm. The data are presented as the mean ± standard error of the mean (n=7). *P<0.05. CTRL, control; NS, not significant; p, phosphorylated; Pio, pioglitazone; PPARγ, peroxisome proliferator-activated receptor γ; UUO, unilateral ureteral obstruction.
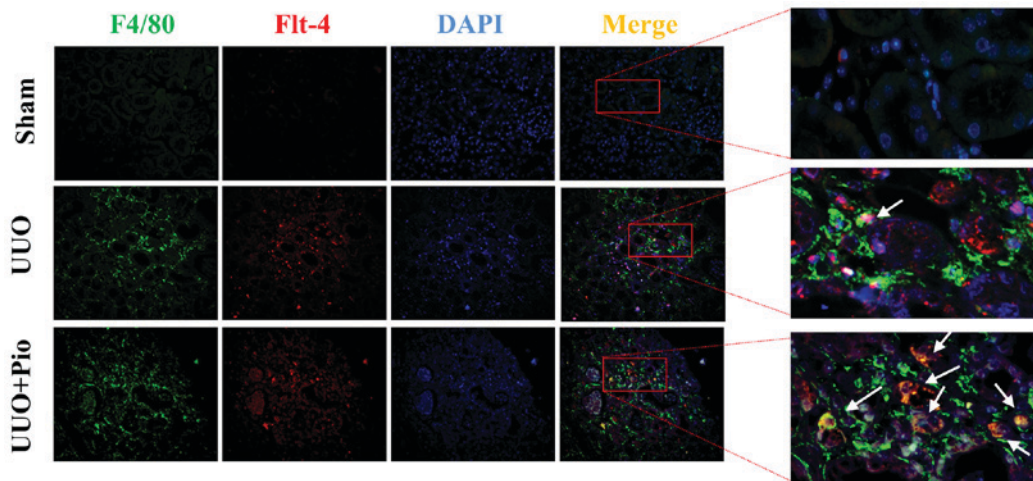

Figure 6. Effect of pioglitazone on the expression of F4/80 and VEGFR3 *in vivo*. Immunofluorescence analysis of F4/80 and VEGFR3 co-localization (white arrows) in kidney sections from mice in the sham, UUO and UUO + pioglitazone groups. Pio, pioglitazone; UUO, unilateral ureteral obstruction; VEGFR3, vascular endothelial growth factor receptor 3.

Vascular endothelial growth factor C (VEGF-C) and its receptor, VEGFR3, also known as Fms related tyrosine kinase 4, are the central pathway for proliferation, migration and survival of lymphatic endothelial cells (LECs) (23). A previous study indicated that the VEGF-C/VEGFR-3 axis serves a vital role in not only LECs, but also a variety of
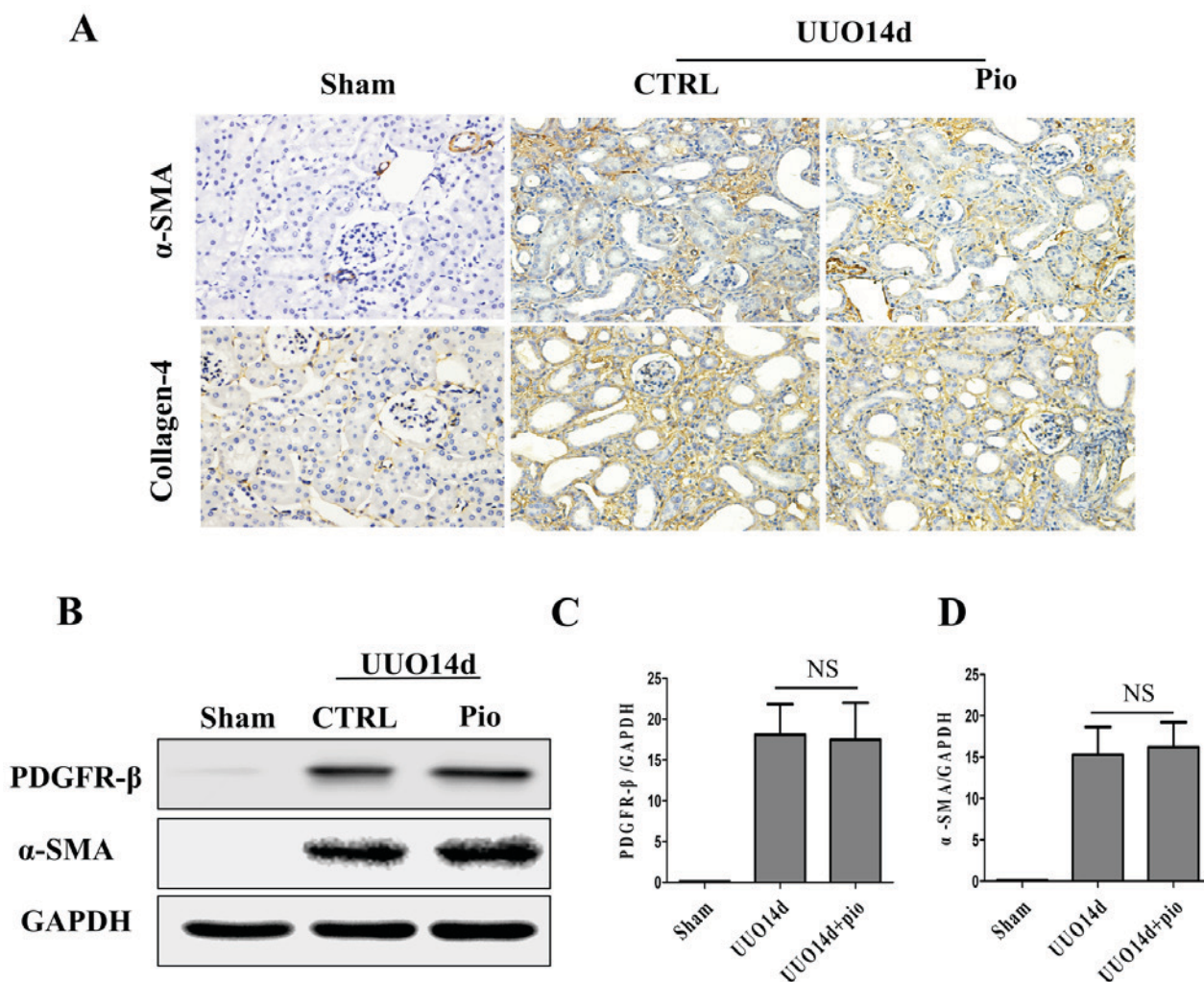
Figure 7. Pioglitazone has no therapeutic effect on renal fibrosis in chronic kidney disease. (A) Immunohistochemical staining of fibrosis markers, α-SMA and collagen-4, in kidney tissues of mice in the sham, UUO and UUO + pioglitazone groups. Scale bar, 100 μm. (B) Western blot analysis was performed to determine the protein expression levels of fibrosis markers, PDGFR-β and α-SMA, in kidney tissues of mice in the sham, UUO and UUO + pioglitazone groups. GAPDH was used as the loading control. (C and D) Quantification of the western blot results. The data are presented as the mean ± standard error of the mean (n=7). α-SMA, α-smooth muscle actin; CTRL, control; NS, not significant; PDGFR-β, platelet-derived growth factor receptor-β; Pio, pioglitazone; UUO, unilateral ureteral obstruction.

other cells, including tumor cells, DCs and macrophages (24). Previous studies have also reported the beneficial effects of the VEGF-C/VEGFR3 pathway in mediating M0 polarization to M1/M2 and ameliorating experimental inflammatory bowel disease (25,26). However, VEGFR3 in macrophages in the context of renal fibrosis requires further investigation. To the best of our knowledge, the present study revealed for the first time that treatment of M2 cells with pioglitazone increased the expression levels of VEGFR3 via a PPARγ-dependent pathway. However, the effect of pioglitazone on renal fibrosis remains unclear.

PPARγ has an important role in regulating metabolic homeostasis, and pioglitazone has been reported to induce activation of PPARγ and exert anti-inflammatory effects (27,28). As a type of antidiabetic drug, PPARγ agonists not only serves a reno-protective role in diabetic nephropathy but also has potential therapeutic effects in non-metabolic kidney disease (29). A previous study reported that pioglitazone treatment serves a potential protective role in non-metabolic nephropathy, such as aging-related progressive renal

injure (30). In experimental mammal kidney disease studies, pioglitazone prevented the NF-κB activation and reduced the kidney damage in cisplatin-treated mice (12), attenuated renal ischemia-reperfusion injury through its anti-inflammation effect (31) and decrease the renal cyst growth in a rat model of polycystic kidney disease (32). However, the effect of pioglitazone on renal fibrosis is limited and controversial (33-35). A recent study reported that pioglitazone protects against renal fibrosis in 5/6 nephrectomized rats (36). Conversely, in our previous study pioglitazone failed to attenuate non-diabetic UUO-induced renal fibrosis, although it partially regulated CD4^{+} T lymphocyte-associated cytokines (14). In addition, the present study further demonstrated that pioglitazone had no therapeutic effect on renal fibrosis in a UUO model. Recent studies indicated that M2 macrophages may have a pro-fibrotic role and inhibition of M2 macrophages may decrease fibrosis in obstructive nephropathy (37). Therefore, activation of M2 macrophages may explain why pioglitazone failed to attenuate UUO-induced renal fibrosis in the present study.

In conclusion, the present study demonstrated that pioglitazone induced polarization of M0 macrophages to M2 macrophages, which may represent a promising therapeutic target for macrophage related inflammatory disease. In addition, pioglitazone upregulated VEGFR3 expression in M2 macrophages via PPAR-γ. Although pioglitazone had no therapeutic effect on renal fibrosis, further investigations on the role of VEGFR3+ M2 macrophages in renal fibrosis, may provide novel insights and treatment strategies for renal fibrosis.

Acknowledgements

Funding

Availability of data and materials

The datasets used and/or analyzed during the current study are available from the corresponding author on reasonable request.

Authors' contributions

ChZ, YZ, YyL and GX designed the study. CoZ and YZ performed the animal surgeries, and YgL performed image analysis and histology. CoZ wrote the first draft of the manuscript and all authors contributed in revising the manuscript.

Ethics approval and consent to participate

The study was approved by the Ethics Committee of Tongji Hospital, Tongji Medical College, Huazhong University of Science and Technology (Wuhan, China).

Patient consent for publication

Not applicable.

Competing interests

The authors declare that they have no competing interests.

References

1. Ma YC, Zuo L, Chen JH, Luo Q, Yu XQ, Li Y, Xu JS, Huang SM, Wang LN, Huang W, *et al*: Modified glomerular filtration rate estimating equation for chinese patients with chronic kidney disease. J Am Soc Nephrol 17: 2937-2944, 2006.
2. Levey AS, de Jong PE, Coresh J, El Nahas M, Astor BC, Matsushita K, Gansevoort RT, Kasiske BL and Eckardt KU: The definition, classification, and prognosis of chronic kidney disease: A KDIGO controversies conference report. Kidney Int 80: 17-28, 2011.
3. Coresh J, Selvin E, Stevens LA, Manzi J, Kusek JW, Eggers P, van Lente F and Levey AS: Prevalence of chronic kidney disease in the United States. JAMA 298: 2038-2047, 2007.
4. Fogo AB: Mechanisms of progression of chronic kidney disease. Pediatr Nephrol 22: 2011-2022, 2007.
5. Chevalier RL, Forbes MS and Thornhill BA: Ureteral obstruction as a model of renal interstitial fibrosis and obstructive nephropathy. Kidney Int 75: 1145-1152, 2009.
6. Wang Y and Harris DC: Macrophages in renal disease. J Am Soc Nephrol 22: 21-27, 2011.
7. Murray PJ and Wynn TA: Protective and pathogenic functions of macrophage subsets. Nat Rev Immunol 11: 723-737, 2011.
8. Owen MR, Stamper IJ, Muthana M, Richardson GW, Dobson J, Lewis CE and Byrne HM: Mathematical modeling predicts synergistic antitumor effects of combining a macrophage-based, hypoxia-targeted gene therapy with chemotherapy. Cancer Res 71: 2826-2837, 2011.
9. Spitler LE, Grossbard ML, Ernstoff MS, Silver G, Jacobs M, Hayes FA and Soong SJ: Adjuvant therapy of stage III and IV malignant melanoma using granulocyte-macrophage colony-stimulating factor. J Clin Oncol 18: 1614-1621, 2000.
10. Ahmadian M, Suh JM, Hah N, Liddle C, Atkins AR, Downes M and Evans RM: PPARγ signaling and metabolism: The good, the bad and the future. Nat Med 19: 557-566, 2013.
11. Murphy GJ and Holder JC: PPAR-γ agonists: Therapeutic role in diabetes, inflammation and cancer. Trends Pharmacol Sci 21: 469-474, 2000.
12. Zhang J, Zhang Y, Xiao F, Liu Y, Wang J, Gao H, Rong S, Yao Y, Li J and Xu G: The peroxisome proliferator-activated receptor γ agonist pioglitazone prevents NF-κB activation in cisplatin nephrotoxicity through the reduction of p65 acetylation via the AMPK-SIRT1/p300 pathway. Biochem Pharmacol 101: 100-111, 2016.
13. Hontecillas R, Horne WT, Climent M, Guri AJ, Evans C, Zhang Y, Sobral BW and Bassaganya-Riera J: Immunoregulatory mechanisms of macrophage PPAR-γ in mice with experimental inflammatory bowel disease. Mucosal Immunol 4: 304-313, 2011.
14. Zhang Y, Wang J, Zhou QD, Zhang CH, Li Q, Huang S, Zhan J, Wang K, Liu YY and Xu G: Peroxisome proliferator-activated receptor-γ agonist pioglitazone fails to attenuate renal fibrosis caused by unilateral ureteral obstruction in mice. J Huazhong Univ Sci Technol Med Sci 36: 41-47, 2016.
15. Liu Y, Wang K, Liang X, Li Y, Zhang Y, Zhang C, Wei H, Luo R, Ge S and Xu G: Complement C3 produced by macrophages promotes renal fibrosis via IL-17A secretion. Front Immunol 9: 2385, 2018.
16. Ying W, Cheruku PS, Bazer FW, Safe SH and Zhou B: Investigation of macrophage polarization using bone marrow derived macrophages. J Vis Exp, 2013.
17. Duffield JS: Macrophages and immunologic inflammation of the kidney. Semin Nephrol 30: 234-254, 2010.
18. Nikolic-Paterson DJ, Wang S and Lan HY: Macrophages promote renal fibrosis through direct and indirect mechanisms. Kidney Int Suppl (2011) 4: 34-38, 2014.
19. Wang YY, Jiang H, Pan J, Huang XR, Wang YC, Huang HF, To KF, Nikolic-Paterson DJ, Lan HY and Chen JH: Macrophage-to-myofibroblast transition contributes to interstitial fibrosis in chronic renal allograft injury. J Am Soc Nephrol 28: 2053-2067, 2017.
20. Tuccori M, Filion KB, Yin H, Yu OH, Platt RW and Azoulay L: Pioglitazone use and risk of bladder cancer: Population based cohort study. BMJ 352: i1541, 2016.
21. Li H, Sorenson AL, Poczobutt J, Amin J, Joyal T, Sullivan T, Crossno JT Jr, Weiser-Evans MC and Nemenoff RA: Activation of PPARγ in myeloid cells promotes lung cancer progression and metastasis. PLoS One 6: e28133, 2011.
22. Zhu Z, Ding J, Ma Z, Iwashina T and Tredget EE: Alternatively activated macrophages derived from THP-1 cells promote the fibrogenic activities of human dermal fibroblasts. Wound Repair Regen 25: 377-388, 2017.
23. Tammela T and Alitalo K: Lymphangiogenesis: Molecular mechanisms and future promise. Cell 140: 460-476, 2010.
24. Su JL, Yen CJ, Chen PS, Chuang SE, Hong CC, Kuo IH, Chen HY, Hung MC and Kuo ML: The role of the VEGF-C/VEGFR-3 axis in cancer progression. Br J Cancer 96: 541-545, 2007.
25. D'Alessio S, Correale C, Tacconi C, Gandelli A, Pietrogrande G, Vetrano S, Genua M, Arena V, Spinelli A, Peyrin-Biroulet L, *et al*: VEGF-C-dependent stimulation of lymphatic function ameliorates experimental inflammatory bowel disease. J Clin Invest 124: 3863-3878, 2014.

26. Beghdadi W, Madjene LC, Claver J, Pejler G, Beaudoin L, Lehuen A, Daugas E and Blank U: Mast cell chymase protects against renal fibrosis in murine unilateral ureteral obstruction. Kidney Int 84: 317-326, 2013.
27. Sugawara A, Uruno A, Kudo M, Matsuda K, Yang CW and Ito S: Effects of PPARγ on hypertension, atherosclerosis, and chronic kidney disease. Endocr J 57: 847-852, 2010.
28. Rosen ED and Spiegelman BM: PPARgamma: A nuclear regulator of metabolism, differentiation, and cell growth. J Biol Chem 276: 37731-37734, 2001.
29. Fogo AB: PPARγ and chronic kidney disease. Pediatr Nephrol 26: 347-351, 2011.
30. Yang HC, Deleuze S, Zuo Y, Potthoff SA, Ma LJ and Fogo AB: The PPARgamma agonist pioglitazone ameliorates aging-related progressive renal injury. J Am Soc Nephrol 20: 2380-2388, 2009.
31. Singh AP, Singh N and Bedi PM: Pioglitazone ameliorates renal ischemia reperfusion injury through NMDA receptor antagonism in rats. Mol Cell Biochem 417: 111-118, 2016.
32. Blazer-Yost BL, Haydon J, Eggleston-Gulyas T, Chen JH, Wang X, Gattone V and Torres VE: Pioglitazone attenuates cystic burden in the PCK rodent model of polycystic kidney disease. PPAR Res 2010: 274376, 2010.
33. Ochodnicky P, Mesarosova L, Cernecka H, Klimas J, Krenek P, Goris M, van Dokkum RP, Henning RH and Kyselovic J: Pioglitazone, a PPARγ agonist, provides comparable protection to angiotensin converting enzyme inhibitor ramipril against adriamycin nephropathy in rat. Eur J Pharmacol 730: 51-60, 2014.
34. Higashi K, Oda T, Kushiyama T, Hyodo T, Yamada M, Suzuki S, Sakurai Y, Miura S and Kumagai H: Additive antifibrotic effects of pioglitazone and candesartan on experimental renal fibrosis in mice. Nephrology (Carlton) 15: 327-335, 2010.
35. Han JY, Kim YJ, Kim L, Choi SJ, Park IS, Kim JM, Chu YC and Cha DR: PPARgamma agonist and angiotensin II receptor antagonist ameliorate renal tubulointerstitial fibrosis. J Korean Med Sci 25: 35-41, 2010.
36. Sun L, Yuan Q, Xu T, Yao L, Feng J, Ma J, Wang L, Lu C and Wang D: Pioglitazone improves mitochondrial function in the remnant kidney and protects against renal fibrosis in 5/6 nephrectomized rats. Front Pharmacol 8: 545, 2017.
37. Nishida M and Hamaoka K: Macrophage phenotype and renal fibrosis in obstructive nephropathy. Nephron Exp Nephrol 110: e31-36, 2008.